PROCEEDINGS OF SCIENCE

Expected performance of the Auger Radio Detector

Felix Schlüter [a,b,1] **on behalf of the Pierre Auger Collaboration** [c,2]

[a] *Karlsruher Institut für Technologie, Institut für Astroteilchenphysik, Karlsruhe, Germany*

[b] *Universidad Nacional de San Martín, Instituto de Tecnologías en Detección y Astropartículas, Buenos Aires, Argentina*

[c] *Observatorio Pierre Auger, Av. San Martín Norte 304, 5613 Malargüe, Argentina*

E-mail: fschluter@icecube.wisc.edu, spokespersons@auger.org

The Auger Radio Detector (RD) will increase the sky coverage and overall aperture for mass-sensitive measurements of ultra-high-energy cosmic rays with the Pierre Auger Observatory. The installation of over 1600 dual-polarized short aperiodic loaded loop antennas (SALLAs) on an area of about 3000 km^2 will enable the detection of highly inclined air showers via the emitted electromagnetic radiation in coincidence with the Auger water-Cherenkov detector array (SD). The combination of complementary information from both detectors yields a strong sensitivity to the mass composition of cosmic rays.

We will present the expected performance of the RD to detect and reconstruct inclined air showers. This study features comprehensive sets of Monte-Carlo generated air showers, utilizes a complete description of the instrumental response of the radio antennas, and in-situ recorded background. The estimation of an energy- and direction-dependent aperture yields an expectation of about 3900 events with energies above 10^{19} eV being detected during 10 years of operation. From a full event reconstruction, we quantify the achievable energy resolution to be better than 10% at and beyond 10^{19} eV. With this at hand, the potential to measure the number of muons and discriminate between different cosmic-ray primaries in combination with the SD using inclined air showers is presented. The discrimination between proton- and iron-induced air showers yields a figure-of-merit of 1.6.

Acoustic & Radio EeV Neutrino Detection Activities (ARENA)
7–10 Jun 2022
Santiago de Compostela, Spain

[1] Speaker
[2] Full author list at http://www.auger.org/archive/authors_2022_06.html.

PoS(ARENA2022)028

1. Introduction

Inclined air showers with zenith angles beyond 60° to 65° can be detected by kilometer-sparse radio-antenna arrays [1]. Such arrays can be upscaled cost effectively to provide a sufficient aperture of $\gtrsim 1000\,\mathrm{km^2 sr}$ to detect cosmic rays at the highest energies from 10^{19} eV to 10^{20} eV. In highly inclined air showers, the electromagnetic cascade is absorbed in the atmosphere and only muons reach the ground. However, radio antennas allow us to measure the electromagnetic radiation from those electrons which is only very weakly correlated with the primary cosmic ray mass and thus enables an unbiased estimation of the cosmic ray energy. In contrast, the muon content of an air shower is strongly correlated with the cosmic ray mass. Hence, combining a radio and particle (muon) detector allows to infer the mass of the primary cosmic ray [2].

With the currently ongoing AugerPrime upgrade [3], the Pierre Auger Observatory is extending the mass-composition sensitivity of its $3000\,\mathrm{km^2}$ large Surface Detector (SD). The upgrade constitutes, among other things, the installation of a $3.8\,\mathrm{m^2}$ scintillator panel on most, and the installation of a dual-polarized short aperiodic loaded loop antenna (SALLA) on all, existing water-Cherenkov detector (WCD) stations. While the WCDs in combination with the scintillator panels provide electron-muon separation due to their different responses to electrons and muons for vertical showers[1], the Radio Detector (RD) in combination with the WCDs[2] provide electron-muon separation for inclined air showers until close to the horizon. Thus the RD increases the overall aperture and sky coverage of mass-sensitive detections with the upgraded observatory. Both aspects are crucial for anisotropy studies.

In this work, we investigate the performance of the RD employing Monte-Carlo (MC) air shower simulations, and a detailed simulation of the instrumental response of the RD. A particular focus is set to answer the following three questions: I) What is the efficiency of the RD to detect air showers and how many air showers will it detect? II) How precisely can we determine the cosmic ray energy for the detected air showers? III) In combination with the SD, how well can we discriminate between light and heavy cosmic rays, e.g., between proton- and iron-induced air showers? For a comprehensive write-up of this analysis see chapter 8 and 9 in [4].

2. The Auger Radio Detector

The Auger Radio Detector will consist of a dual-polarized SALLA antenna mounted on each WCD, yielding a total of 1661 antennas situated on a hexagonal grid with a spacing of 1.5 km. The SALLAs are polarized in the East-West and North-South directions and are, including the subsequent signal processing chain, sensitive to the electromagnetic emission in the 30 to 80 MHz band. The electric field is recorded with a sampling rate of 250 MHz for 8.192 μs with a 12 bit analog-to-digital converter (ADC) once the WCD beneath sends a trigger. The entire signal chain amplifies the signals by $\sim 23.6\,\mathrm{dB}$. For a more detailed description of the technical design of the RD see chapter 3.4 in [4].

Since November 2019, seven station equipped with readout electronics have been deployed on site. Those stations have recorded first air shower signals and ambient as well as electronic noise.

[1] Those measurements are limited to $\theta \lesssim 60°$ as the effective area of the scintillator panels scales with $\cos\theta$.

[2] In the following we refer to as SD although, strictly speaking, the RD is part of the SD as well.

A pilot calibration campaign using the galactic radio emission as a reference signal estimates an absolute gain accuracy of $\sim 10\%$ [5]. For this work we use noise data recorded since September 2021 with updated readout electronics to realistically describe the radio background at the site.

3. Simulating events for the Radio Detector

In order to estimate the expected performance of the Radio Detector as accurately as possible, we have to mimic the data which will be recorded by antennas as realistically as possible. This endeavor can be divided into the simulation of the physics signals arriving at the detector units for a given air shower and the simulation of the instrumental response to those signals. To simulate the particles and radio emission arriving at the ground we used CORSIKA and its radio extension CoREAS [6]. We simulated air showers initiated by proton, helium, nitrogen, and iron primaries with an inclination of $\theta \in [65°, 85°]$ and energy of $E \in [10^{18.4}\,\mathrm{eV}, 10^{20}\,\mathrm{eV}]$. The ambient conditions match those of the Pierre Auger Observatory. To simulate the instrumental response of the WCDs as well as the radio antennas we used the official $\overline{\mathrm{Off}}\underline{\mathrm{line}}$ simulation and reconstruction framework of the Pierre Auger Collaboration. The simulation of the instrumental response of the radio antennas encompasses: the directional sensitivity of the SALLA antennas, signal amplification and attenuation due to the readout via a low-noise amplifier, signal transmission through a cable, filtering with a filter amplifier, and sampling and digitization with the ADC. To the digitized simulated signals we add recorded noise traces. We assume that the sensitivity among different antennas varies by 5% in amplitude, i.e., we apply a Gaussian smearing on the amplitudes of individual antennas by $\sigma_A = 5\%$ prior to digitization. The timing resolution, which is dominated by the GPS clocks, is simulated with $\sigma_t = 6\,\mathrm{ns}$. This procedure is only conducted for air showers which triggered the SD and for antennas with a trigger from the WCD beneath.

4. Expected detection rate with the Radio Detector

Before, determining the detection efficiency and subsequently the event rate, the (simulated) recorded data from the antennas need to be reconstructed. The reconstruction procedure aims to unfold the instrumental response and determine the incoming electric field. For more details see [4, 7]. From the reconstructed electric field traces a signal-to-noise ratio SNR is determined, the energy fluence, i.e., the energy deposit per unit area, is calculated, and the signal arrival time is determined. To estimate the detection efficiency we first have to define a detection criterion. We require at least three antenna stations with a SNR ≥ 10 (see [4, Eq. (8.2)] for definition). A SNR ≥ 10 is found to efficiently suppress the false identification of noise pulses with a signal purity of over 99%. Furthermore, three stations allow inferring first air shower properties such as the arrival direction from radio data alone. However, it should be noted that precise reconstruction of, in particular, the air shower energy is not possible with only three antenna stations.

Now, we count all air showers fulfilling this criterion as a function of their energy and zenith angle and divide them by all showers triggering the SD in the corresponding bin. We use all SD-triggered air showers instead of all simulated air showers to mitigate a lower trigger efficiency of the SD in simulations w.r.t. real observations due to the muon deficit in simulations [8]. Fig. 1 (*left*) shows the detection efficiency for several energy bins (color-coded) as a function of the zenith

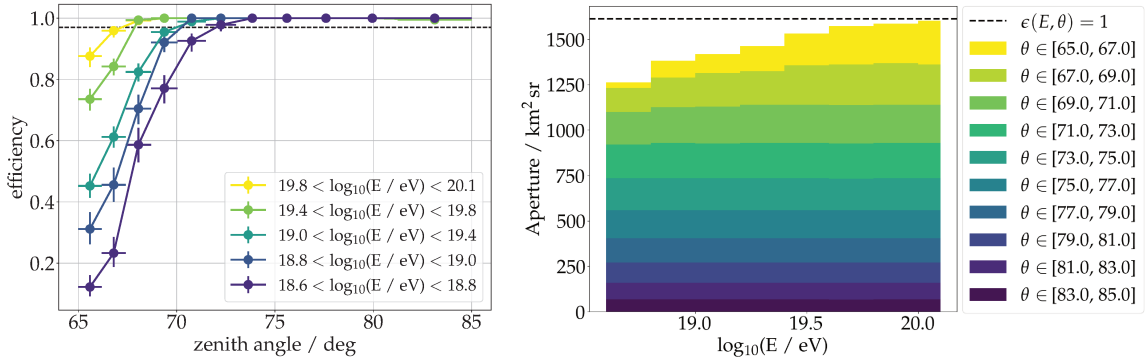

Figure 1: *Left*: Detection efficiency as a function of the zenith angle and cosmic-ray energy (color-coded). The horizontal dashed line indicates an efficiency of 97%. Only statistical uncertainties are shown. *Right*: Stacked histogram of the aperture as a function of the cosmic-ray energy. Each colored layer describes the contribution of a zenith-angle band. At the highest energies the ideal aperture, i.e., the aperture with perfect efficiency, indicated by the horizontal dashed line, is approached.

angle. The uncertainties are estimated using binomial statistics. It is apparent that the efficiency depends more strongly on the zenith angle than on the energy as the size of the footprint increases more strongly with the inclination. Beyond a zenith angle of $\sim 70°$ the RD detects air showers with full efficiency. It should be noted that the efficiency also depends on the azimuth angle which is omitted here. However, we found that this correlation is of second order and in particular does not affect the efficiency at zenith angles beyond $\sim 70°$. The same is true for the different primary types.

The aperture, i.e., the effective area times solid angle, is calculated multiplying the array size with the efficiency ϵ and integrating over the sky. Here, the projection of the flat detector onto the air shower frame is considered with the factor $\cos\theta$. Solving the integral results in the following expression for the aperture $\mathcal{A}(\theta_1, \theta_2, E_1, E_2) = 3000\,\mathrm{km}^2\pi \left[\cos^2\theta_1 - \cos^2\theta_2\right] \epsilon(\theta_1, \theta_2, E_1, E_2)$. Fig. 1 (*right*) shows the aperture in a histogram stacked in zenith angle as function of the energy. It is visible that the relative contribution to the total aperture decreases with the zenith angle, an effect of the projection. An ideal aperture $\mathcal{A}_{\mathrm{ideal}}(\epsilon = 1) = 1612\,\mathrm{km}^2\mathrm{sr}$ is approached at the highest energies as indicated by the dashed horizontal line. The extension of sky coverage with $\theta = 65° - 85°$ increases the aperture by 23% w.r.t. $\theta < 60°$.

The aperture can now be multiplied with the flux of ultra-high-energy cosmic rays and integrated over energy to determine an event rate. For this calculation, we use the most recent flux measurement by Auger [9]. In Fig. 2 we show the event rate for a live time of 10 years once for the entire sky between 65° and 85° (blue) and once for those parts of the sky where the efficiency is $\epsilon(\theta, E) > 97\%$ (red). The event rate is shown as an integral from a lower threshold energy as a function of this energy, i.e., $N(E_{\mathrm{th}}) = N(E \geq E_{\mathrm{th}})$, the uncertainties are statistical only. Those event rates are compared to the number of inclined events detected at Auger in coincidence between the SD and Fluorescence Detector (FD) which allow for similar studies as SD-RD hybrid events [10], and of all-sky events detected by several experiments around the world using fluorescence telescopes [11]. We expect to detect 3925^{+62}_{-102} air showers for energies above 10^{19} eV in 10 years. We varied several parameters in the air shower simulations as well as detector simulation such as changing the hadronic interaction model, atmospheric conditions, particle thinning, and absolute antenna sensitivity. For

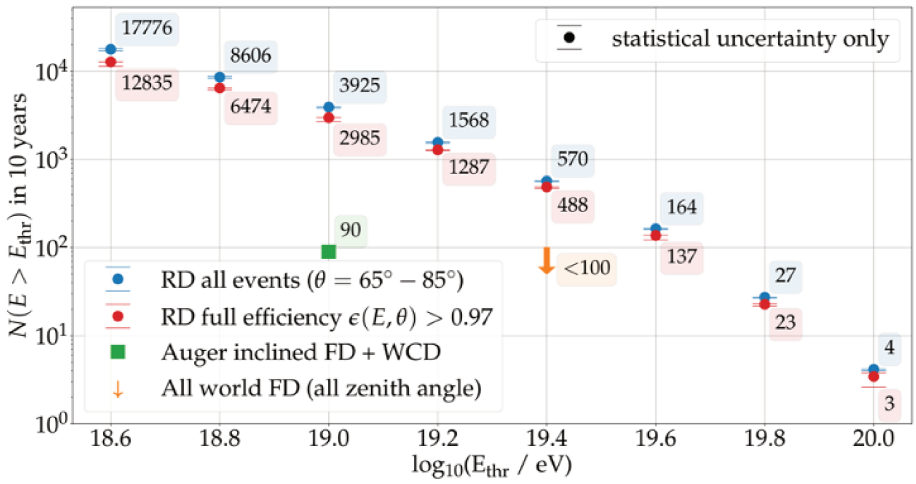

Figure 2: Integrated number of events for 10 years of live time as a function of the lower energy threshold. The event rate is shown for the entire zenith angle range (blue) and only for those angles with an efficiency $\geq$ 97% (red). Presented uncertainties are purely statistical. Those results are compared to more than 10 years of inclined hybrid events between the Auger SD and FD [10] and the number of the very-high-energy cosmic ray events recorded with several Fluorescence detectors so far [11].

energies above 10^{19} eV we found those systematic effects to be lower than or on the same level as the statistical uncertainty.

5. Expected energy resolution for the Radio Detector

To reconstruct the shower energy we use a newly developed signal model, i.e., a lateral distribution function (LDF) of the radio emission, to describe the reconstructed energy fluences as a function of the electromagnetic shower energy $E_{\rm em}$ and geometrical distance between the ground and the shower maximum along the shower axis $d_{\rm max}$. A comprehensive description and evaluation of the signal model can be found in [12]. We derive an initial guess for the fit parameters from the SD-reconstructed energy and an arrival direction determined using radio data and a spherical wavefront model. To evaluate the performance of the reconstruction we select only showers with a minimum zenith angle of $\theta \geq 68°$ and at least five signal stations. The latter allows us to determine the core position together with the two fit parameter while maintaining a degree of freedom. We employ further quality cuts to ensure, among other things, a sufficient sampling of the LDF and good fit quality. The efficiency of these quality cuts is above 95%. The result of the reconstruction is shown in Fig. 3, once as a scatter plot (*left*) reconstructed vs true electromagnetic energy, and once as a histogram of reconstructed over true electromagnetic energy. In the left panel it is visible that the spread decreases, i.e., the accuracy improves, with energy. This is expected due to the influence of noise on the signal reconstruction. In the right panel the result integrated over all energies but separated by the different primaries is shown. While no significant bias and a very good energy resolution of $\sigma_{E_{\rm em}} \sim 6\%$ is found, no significant difference for the different primaries is apparent. Those results are important, in particular for the separation of different primaries. To convert the electromagnetic shower energy to a total-shower or cosmic-ray energy $E_{\rm CR}$ we apply a linear

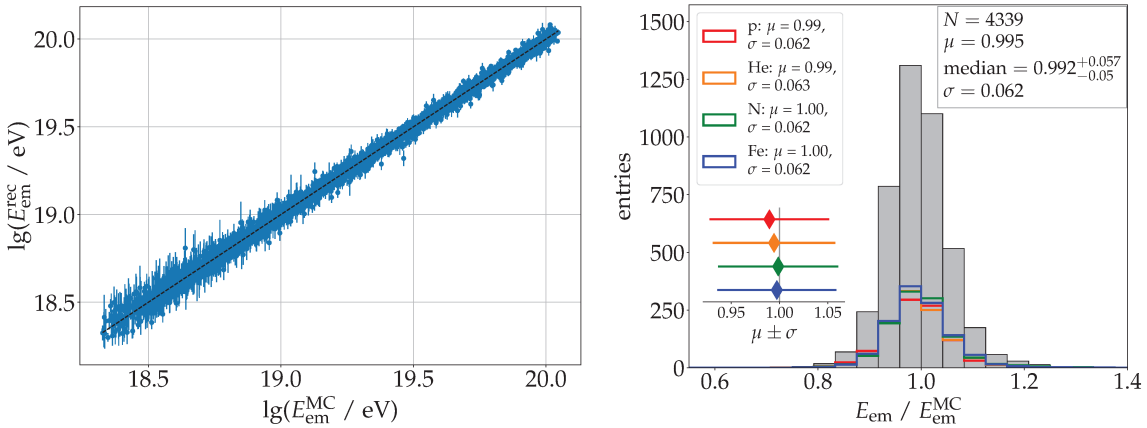

Figure 3: *Left*: Scatter plot of the reconstructed electromagnetic shower energy as a function of the true energy for all showers passing our selection. The dashed line indicates the diagonal. *Right*: Histogram of the ratio of the reconstructed electromagnetic shower energy over the true electromagnetic energy. The colored lines indicate the distribution for a particular primary. The legend displays the resolution and bias.

calibration which was found using simulations: $E_{\rm CR} = E_{\rm em} \cdot \left[1.1426 - 0.0328 \log_{10}(E_{\rm em}/10\,{\rm EeV})\right]$. It should be noted that this calibration is independent of the primary particle mass which introduces a mass dependent bias into the reconstructed cosmic-ray energy. Hence, the electromagnetic shower energy is better suited to discriminate between different primaries.

6. Expected mass sensitivity of hybrid detection with AugerPrime using inclined air showers

To correctly estimate the potential of hybrid detection with the RD and SD, we have to reweight our set of simulations to match what is expected from nature. This concerns three parameters: arrival direction distribution, energy spectrum and mass composition. The former is already simulated as expected from nature. The energy spectrum is reweighted according to the event rate determined in Sec. 4, this reweighting provokes that lower energy showers in our simulation set are used multiple times. As the mass composition is highly uncertain, we use two competing scenarios, the so-called "maximum-rigidity" and "photo-disintegration" scenarios, as well as an unrealistic 50-50 proton iron mix to test the discriminative power of those measurements. While the maximum-rigidity model describes a mass composition which becomes gradually heavier with energy, the photo-disintegration scenario predicts a lighter composition which is dominated by nitrogen at the highest energies. For more information on both scenarios see [3].

First, we evaluate the discriminative power using the RD-reconstructed electromagnetic shower energy $E_{\rm em}$ and the SD-reconstructed number of muons R_μ. R_μ is a dimensionless observable representing the muon content of the air shower relative to the muon content of a simulated 10^{19} eV proton shower with the same zenith angle, for more details on the SD reconstruction see [13]. To separate proton- from iron-induced air showers, we normalize R_μ by $(E_{\rm em}/10\,{\rm EeV})^{0.91}$ to remove the non-linear energy scaling of R_μ. Furthermore, to avoid any bias due to different reconstruction efficiencies for the different primaries and to improve the overall discrimination, we only select showers with a reconstructed $\theta \geq 70^\circ$ and $E_{\rm em} \geq 10^{19}$ eV. Figure 4 (*left*) shows $r = R_\mu/(E_{\rm em}/10\,{\rm EeV})^{0.91}$

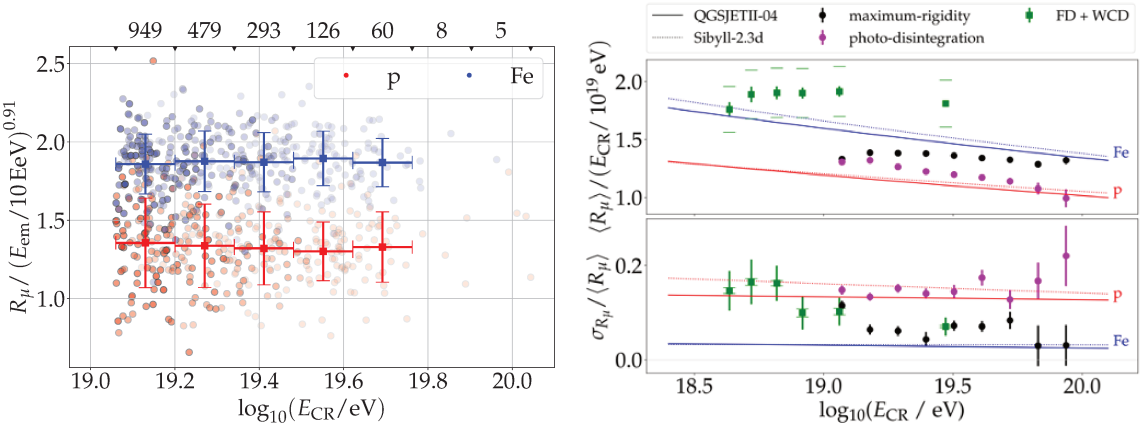

Figure 4: *Left*: Scatter plot of $r = R_\mu/(E_{em}/10\,\mathrm{EeV})^{0.91}$ as a function of the RD-reconstructed total cosmic ray energy. Proton and iron induced showers are colored individually. The transparency of the markers resamples their weight, i.e., their frequency, in the reweighed data set. The squared marker show mean and standard deviation in bins with more than 10 entries (see top x-axis). *Right*: Mean number of muons (top) and physical fluctuation of the number of muon (bottom) for: simulated measurements with the RD and SD of two competing mass-composition scenarios, measurement of the FD and SD from [10] (green), MC predictions of pure proton and iron beams for different hadronic interaction models (lines).

as a function of the RD-reconstructed total cosmic ray energy for proton showers colored in red and iron showers colored in blue. A clear separation between the proton- and iron-induced air showers is visible with iron showers containing on average more muons than proton showers. We can quantify the separation with the figure of merit: $\mathrm{FOM} = |\langle r_p \rangle - \langle r_{Fe} \rangle| / \sqrt{\sigma^2_{r_p} + \sigma^2_{r_{Fe}}} = 1.60 \pm 0.05$. Keep in mind, that this FOM is obtained using a realistic continuous and steep energy spectrum. The uncertainty is obtained by evaluating the standard deviation of the FOM distribution of a 1000 randomly drawn event sets. To bring this into perspective, a separation of those primaries using X_{max} requires a nearly perfect detector resolution with $\sigma_{X_{max}} < 10\,\mathrm{g\,cm^{-2}}$ which is not achieved by state-of-the-art Fluorescence Detectors such as the one of the Pierre Auger Observatory.

The mean number of muons $\langle R_\mu \rangle(E)$ as a function of the energy as well as their physical fluctuations $\sigma_{R_\mu}/\langle R_\mu \rangle$ can also be used to determine the (mean) mass composition of ultra-high-energy cosmic rays. To determine σ_{R_μ}, one has to determine the variance of R_μ and subtract the square of the detector resolutions for both R_μ and E_{CR}[3]. Fig. 4 (*right*) shows the mean number of muons on top and physical fluctuations on the bottom panel as a function of the cosmic-ray energy. The simulated measurements of the RD-SD for the two different mass-composition scenarios are compared to the prediction of pure proton and iron beams for different hadronic interaction models (lines) and a measurement of the Pierre Auger Observatory with the SD and FD (green)[4]. It is obvious that the RD will allow us to extend the existing measurements at Auger to higher energies and with higher statistical power[5]. Although systematic uncertainties likely prohibit determining the average mass composition using the mean number of muons, the physical fluctuations which are

[3]This procedure is only strictly correct if R_μ scales linearly with E_{CR} and their resolutions are uncorrelated.

[4]The disagreement between the measurement and MC predictions is due to the muon deficit in simulations.

[5]For the RD results only statistical uncertainties are shown, as a first estimate we can assume similar systematic uncertainties as for the FD-SD measurement (green error caps).

much less affected by systematic effects promises to allow for a clear separation between different astrophysical mass-composition scenarios.

7. Conclusion

We presented results of an end-to-end, Monte-Carlo powered simulation study of hybrid detection with the Radio Detector and (particle) Surface Detector of the upgraded Pierre Auger Observatory. A full characterization of the performance of the RD in terms of the accessible event rate and achievable energy resolution has been performed demonstrating that I) the available statistics with $\sim$ 3900 detected events above 10^{19} eV will improve on that of comparable measurements (inclined FD-SD hybrid events) by more than one order of magnitude, and II) the estimated energy resolution is with $\sim$ 6%, given current assumptions about the detector, very promising. With those results the potential of RD-SD hybrid events to separate between air showers initiated by different primaries, and to determine the average mass composition of ultra-high-energy cosmic rays, has been studied. It was found that RD-SD events provide a very competitive separation power with a Figure-of-Merit = 1.6 and the potential to discriminate between different astrophysical mass-composition scenarios.

References

[1] Pierre Auger, *Measurements of Inclined Air Showers with the Auger Engineering Radio Array at the Pierre Auger Observatory*, *PoS* **ICRC2019** (2021) 274.

[2] E.M. Holt, F.G. Schröder and A. Haungs, *Enhancing the cosmic-ray mass sensitivity of air-shower arrays by combining radio and muon detectors*, *Eur. Phys. J.* **C79** (2019) 371 [1905.01409].

[3] Pierre Auger, *The Pierre Auger Observatory Upgrade - Preliminary Design Report*, 1604.03637.

[4] F.A. Schlüter, *Expected sensitivity of the AugerPrime Radio Detector to the masses of ultra-high-energy cosmic rays using inclined air showers*, Ph.D. thesis, KIT, Karlsruhe, IAP, 2022. https://publikationen.bibliothek.kit.edu/1000149113.

[5] Pierre Auger, *First results from the AugerPrime Radio Detector*, *PoS* **ICRC2021** (2021) 270.

[6] T. Huege, M. Ludwig and C.W. James, *Simulating radio emission from air showers with CoREAS*, *AIP Conf. Proc.* **1535** (2013) 128.

[7] Pierre Auger, *Energy Estimation of Cosmic Rays with the Engineering Radio Array of the Pierre Auger Observatory*, *Phys. Rev. D* **93** (2016) 122005 [1508.04267].

[8] J. Albrecht et al., *The Muon Puzzle in cosmic-ray induced air showers and its connection to the Large Hadron Collider*, *Astrophys. Space Sci.* **367** (2022) 27 [2105.06148].

[9] Pierre Auger, *Measurement of the cosmic -ray energy spectrum above* 2.5×10^{18} *eV using the Pierre Auger Observatory*, *Phys. Rev. D* **102** (2020) 062005 [2008.06486].

[10] Pierre Auger, *Measurement of the fluctuations in the number of muons in extensive air showers with the pierre auger observatory*, *Phys. Rev. Lett.* **126** (2021) 152002 [2102.07797].

[11] A. Coleman et al., *Ultra-High-Energy Cosmic Rays: The Intersection of the Cosmic and Energy Frontiers*, 2205.05845.

[12] F. Schlüter and T. Huege, *Signal model and event reconstruction for the radio detection of inclined air showers*, 2203.04364.

[13] Pierre Auger, *Reconstruction of Inclined Air Showers detected with the Pierre Auger Observatory*, *JCAP* **08** (2014) 019 [1407.3214].